

RESEARCH ARTICLE

Derivation of aerial insect concentration with a 94 GHz FMCW cloud radar

Moritz Lochmann*¹ | Heike Kalesse-Los¹ | Birgen Haest² | Teresa Vogl¹ | Roel van Klink^{3,4} | Freya Addison¹ | Maximilian Maahn¹ | Willi Schimmel⁷ | Christian Wirth^{3,5,6} | Johannes Quaas^{1,3}

¹Leipzig Institute for Meteorology, Leipzig University, Leipzig, Germany

²Swiss Ornithological Institute, Sempach, Switzerland

³German Centre for Integrative Biodiversity Research (iDiv) Halle Jena Leipzig, Leipzig, Germany

⁴Department of Computer Science, Martin Luther University-Halle Wittenberg, Halle (Saale), Germany

⁵Systematic Botany and Functional Biodiversity, Leipzig University, Leipzig, Germany

⁶Max-Planck Institute for Biogeochemistry, Jena, Germany

⁷Leibniz Institute for Tropospheric Research (TROPOS), Leipzig, Germany

Correspondence

*Moritz Lochmann, Universität Leipzig, Leipziger Institut für Meteorologie, Stephanstraße 3, 04103 Leipzig, Germany.
Email: moritz.lochmann@uni-leipzig.de

Abstract

Aerial insects are vital for nature and society. Though methods to observe flying insects have consistently improved in the last decades, insects remain difficult to monitor systematically and consistently over large spatial and temporal scales. Remote sensing with radars has proved to be one of the more effective tools for observation. However, as radars are most sensitive to targets similar in size to the radar wavelength, the detectable sub-group of aerial insects of a certain size range depends on the employed radar. Here, we present a novel method based on data of a zenith-pointing W-band (94 GHz, $\lambda = 0.32$ cm) Doppler cloud radar to estimate insect concentration in a vertical profile. Multiple meteorological state-of-the-art algorithms are combined to extract insect signals from the radar data and quantify their abundance from 50 m to 1000 m above the ground. For evaluation, this method is applied to Doppler cloud radar data from a summertime 30 day observation period in central Germany. Results are compared to data from an X-band (9.4 GHz, $\lambda = 3.2$ cm) radar in the same region. Aerial insect concentration derived from the W-band radar, which is sensitive to insects in the mm size range, is substantially higher than from the X-band radar, detecting insects in the cm size range. In addition, diel flight timings vary between the different sub-groups of aerial insects observed by the two radar instruments. With its superior sensitivity to smaller insects like aphids, the proposed methodology complements existing entomological radar techniques and contributes to achieving a more complete description of aerial insect activity.

KEYWORDS

insect detection, radar, retrieval, remote sensing

1 | INTRODUCTION

Over the past decades, multiple studies have reported strong declines in insect population sizes (Thomas et al. 2004), abundances (e.g., Schuch et al. 2012, van Klink et al. 2020) and biomass (Hallmann et al. 2017). Most of these studies have relied on the trapping of insects and subsequent identification of the trapped individuals. Particularly, for aerial insects, trapping by means of Malaise, suction or flight interception traps has been used as standard (Montgomery et al. 2021). However, the data from such traps only represents the aggregated insect assemblage over a certain sampling period (usually a week or more), and for an unknown sampling area, and thus the temporal distribution of insect activity is limited. In addition, the processing of the trapped insects is extremely laborious and, hence, there is a growing need for non-invasive, low maintenance methods for measuring changes in insect abundance, biomass and movement (Chapman et al. 2011).

A variety of methods have been introduced to automatically monitor insects during flight. Insects have been observed by video cameras (Riley 1994), optical sensors (Reynolds and Riley 2002) and lidar instruments (Shaw et al. 2005, Chen et al. 2024),

but radar has proved to be one of the most effective tools for observing insect flight (Drake and Reynolds 2012). As remote-sensing instrumentation, radars operate in a stand-alone way and on a time resolution usually ranging between seconds (cloud radars, BirdScan radars) to minutes (weather radars). In addition, radars allow to sample an entire vertical column. Scanning radars further have the potential to cover spatially large regions. During recent years, the deployment of specialized radar-based detection methods for aerial fauna has become more prevalent, especially for movements of up to several hundred meters up in the air (e.g., Hu et al. 2016, Lukach et al. 2022, Wainwright et al. 2023, Haest et al. 2024b, Bauer et al. 2024). To study larger flying animals, like birds and bats, radar instruments with wavelengths of a few up to several centimeters, like X-band ($\lambda = 2.5\text{-}3.75$ cm; e.g. Giuntini et al. 2024, Werber et al. 2023), C-Band ($\lambda = 4\text{-}8$ cm; e.g. Boero et al. 2020, Nilsson et al. 2019), S-Band ($\lambda = 7.5\text{-}15$ cm; e.g. Haest et al. 2021, Van Doren and Horton 2018), and L-band ($\lambda = 15\text{-}30$ cm; e.g. Weisshaupt et al. 2017) are ever-increasingly used. As radars are most sensitive to targets that are comparable in size to their wavelength, radar instruments operating at lower wavelengths are likely more useful for the detection of aerial insects (Drake et al. 2017). S-band, and more rarely also C-Band (Mäkinen et al. 2022), weather radars have been shown useful to study high-density insect movements (Tielens and Kelly 2024), including specific events like mayfly emergences (Stepanian et al. 2020, Kwakye et al. 2023). X-Band radars have repeatedly been shown useful to study larger individual insects (Chapman et al. 2011, Hu et al. 2016, Gao et al. 2020, Haest et al. 2024b, Bauer et al. 2024), but mostly miss insects with smaller radar cross sections (Riley 1985), which, in fact, are often more abundant. Ku-Band ($\lambda = 1.67\text{-}2.4$ cm), K-Band ($\lambda = 1.11\text{-}1.67$ cm) and Ka-Band ($\lambda = 0.75\text{-}1.11$ cm) radars have seen some use for entomological purposes (e.g., Cai et al. 2019, Zhang et al. 2019), however, almost no studies have been published on W-Band radar insect detection.

In this study, we present a new aerial insect detection method based on observations from a W-Band ($\lambda = 0.32$ cm) Doppler cloud radar, which has the benefit of being able to detect smaller insects in the size range of, e.g., aphids and mosquitoes. A machine learning approach is used to classify insects by exploiting radar Doppler spectra signatures. Additionally, the observations are evaluated in comparison to the data products of a nearby BirdScan MR1 X-Band radar, which is also used for the observation of flying insects, but is more sensitive to larger insects, like moths (e.g., Knop et al. 2023, Haest et al. 2024b). We showcase how knowledge about the behaviour of smaller insects derived from W-Band radar data can complement the already established methods using X-Band radar observations. W-Band radars are already widely used research instruments and most data are publicly available, which represents a worthwhile opportunity to study aerial insects with them. In the meteorological research community, multiple retrievals have been developed to distinguish different target particles detected by radars (e.g., Illingworth et al. 2007, Luke et al. 2008, Radenz et al. 2019, Williams et al. 2021, Schimmel et al. 2022). Here, we explore how to effectively combine different established and state-of-the-art radar data processing techniques to achieve novel results in an aeroecological context.

2 | INSTRUMENTS AND SOFTWARE TOOLS

This section introduces the two radar instruments used in this study, LIMRAD94 and BirdScan MR1. The former provides the data set for the novel insect detection and analysis, while the latter provides a reference data set for validation. Subsequently, the utilized software tools for flying insect detection from the LIMRAD94 radar are presented individually. The algorithm chain of CloudnetPy (Sect. 2.3) is used to create target classification labels for the training of the supervised machine learning model VOODOO. VOODOO (Sect. 2.4) is used to detect signals caused by insects in the cloud radar Doppler spectra. Subsequently, the radar Doppler peak detection algorithms PEAKO (Sect. 2.5) and peakTree (Sect. 2.6) are used to extract information on insect quantities and properties. Section 3.1 details how these software tools are applied to LIMRAD94 data (Sect. 2.1) to detect insects.

2.1 | Doppler cloud radar LIMRAD94

Leipzig University's W-Band Doppler cloud radar LIMRAD94 used in this study is a 94 GHz frequency modulated continuous wave dual-polarization (RPG-FMCW-94-DP) instrument developed for meteorological applications (Küchler et al. 2017, Schimmel et al. 2022). For the purpose of this study, LIMRAD94 was operated from 7 March 2022 to 30 June 2022 at the Leibniz Institute for Tropospheric Research (TROPOS, 51°21' N, 12°26' E) in the Northeastern part of Leipzig, Germany. For this FMCW radar, the transmitted frequency is modulated slightly (300–3600 kHz) around the center frequency of 94 GHz to continuously sample the atmosphere above the instrument in multiple layers, so-called chirps (Küchler et al. 2017). The user can set most of the measurement parameters for each chirp individually in the chirp table configurator. Continuous measurements

with a focus on cloud and insect investigations were performed in June 2022 and the 'cloud' chirp configuration and the 'insect' chirp configuration with lower first range gate and higher vertical resolution have been alternated. Table 1 shows the most relevant measurement parameters for the data set analyzed here for both chirp configurations.

measurement parameter	'cloud' chirp 1	'cloud' chirp 2	'insect' chirp 1	'insect' chirp 2
integration time (s)	0.52	1.77	1.5	0.71
range (m)	100-1200	1200-7000	47.7-417.4	429.3-2000
range resolution (m)	29.8	44.7	11.9	11.9
Nyquist velocity (m s^{-1})	9.0	6.3	8.6	7.8
Doppler velocity resolution (m s^{-1})	0.07	0.05	0.07	0.06
number of Doppler bins	256	256	256	256

TABLE 1 LIMRAD94 chirp settings for the first two chirps for the two used radar chirp sequence settings labeled 'cloud' and 'insect'.

2.2 | BirdScan MR1

The BirdScan MR1 is a pulsed 9.4 GHz radar (X-Band) to track the movement of birds, bats and insects (Shi et al. 2021, Knop et al. 2023, Weisshaupt et al. 2023). The MR1 data used in this study were collected at the research station of the UFZ Helmholtz Centre for Environmental Research in Bad Lauchstädt, Germany (51°23' N, 11°52' E). The instrument was operated from March to October 2022, however, only the overlap period with the continuous measurements of LIMRAD94 (June 2022) is considered here. The MR1 has different operation modes using different pulse lengths with and without rotating the Horn antenna. For each detected object, the probability to be an insect, as one of various sub-groups of biological and non-biological targets, is calculated. If this probability exceeds 0.4 and is higher than for the other sub-groups, it was retained as an insect for further processing. Data were recorded using the short-pulse mode (65 ns pulse length) with a nutating antenna (Haest et al. 2024b). For insects flying through the MR1 beam, their reflecting echo is tracked during their crossing of the beam, and are then stored as individual insects. From these, the hourly aerial density (number of insects per km^3) was then calculated using the birdscanR R package (Haest et al. 2024a) to enable comparison with the insect densities derived from the LIMRAD94 radar data (see Sect. 3.1). An extensive description of the technical details of the MR1 radar can be found in Schmid et al. (2019). Table 2 shows the configuration of both radar instruments and their characteristics. A more detailed description how the differences between the two instruments affect their capacity to detect flying insects can be found in Sect. 3.2.

2.3 | CloudnetPy

The Cloudnet project is part of the Aerosol, Clouds and Trace Gases Research Infrastructure (ACTRIS) and provides a systematic characterization of atmospheric targets by analyzing continuous ground-based observations of the vertical profiles of the atmosphere (Illingworth et al. 2007). Utilizing synergistic effects between Doppler cloud radar (for observation of hydrometeors),

	LIMRAD94	MR1
location	Leipzig, Germany	Bad Lauchstädt, Germany
deployment period	Mar 8 - July 1, 2022	Feb 22 - Oct 31, 2022
center frequency	94 GHz	9.4 GHz
temporal resolution	3 s / 5 s	continuous
vertical resolution	12 m / 30 m	7.5 m
max. considered range	1000 m	500 m
wavelength	0.32 cm	3.2 cm
beam width	0.48°	17.5°

TABLE 2 Comparison of radar instrument specifications of LIMRAD94 and MR1. When two values are given for LIMRAD94, they refer to the different chirp sequence settings 'insects' and 'cloud', respectively.

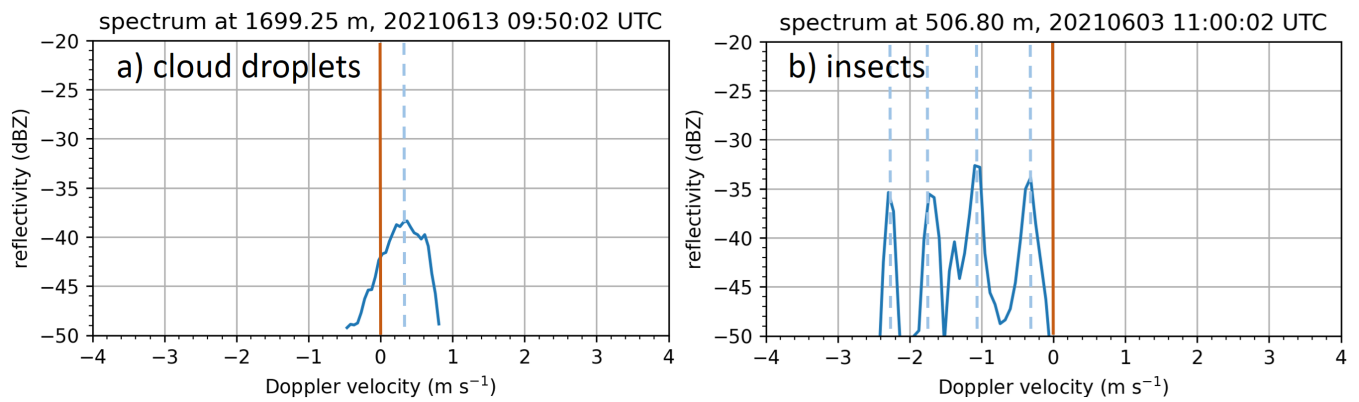


FIGURE 1 Comparison of typical LIMRAD94 radar Doppler peak spectrum between a liquid cloud (left) and insect echoes (right). The presence of liquid water in the left case is determined by supplementary measurements from a ceilometer. The cloud droplets appear as one slightly broader peak close to 0 m s⁻¹, while the insects appear as individual peaks at various Doppler velocities. Negative Doppler velocity values indicate a motion toward the radar (downward) and positive values a motion away from the radar (upward). The dashed blue vertical lines represent Doppler spectrum peaks found by PEAKO.

backscatter lidar (for observation of aerosol particles and cloud base height) and microwave radiometer instruments (for atmospheric temperature and humidity profiling) in combination with atmospheric model data, Cloudnet is able to label the target particles at each point of the vertical profile into different classes. These classes include, e.g., ice, liquid, aerosol, insects and combinations of those.

The CloudnetPy processing toolbox (Tukiainen et al. 2020) provides a Python implementation of the full Cloudnet processing chain. The insect detection in CloudnetPy uses probability functions based on empirical thresholds of temperature and radar variables. Cumulative probability distribution functions depending on the empirically chosen center values (mean value of the distribution) and scales (width of the distribution) are calculated for each of these threshold values.

There are two options for assessing the insect probability within CloudnetPy. The first option is based on the linear depolarization ratio (LDR) which is the ratio of cross- to co-channel reflectivity and gives information about the targets shapes. If LDR is available, the variables used for determining the insect probability are LDR and wet bulb temperature in the considered altitude from ancillary weather model data. The individual insect probability for both of these variables is calculated and multiplied to get the combined insect probability. This method is generally considered the best proxy for insect detection (Tukiainen et al. 2020). However, the LDR value is not always available, e.g. because of low signal to noise ratios. In that case, the alternative variables used to calculate the insect probability are the integrated radar Doppler spectra data (moments) being radar reflectivity, mean Doppler velocity, Doppler spectral width as well as wet bulb temperature. Both approaches largely depend on the empirically chosen threshold values for the radar variables. If the insect probability by either of these two approaches exceeds the CloudnetPy threshold of 0.8, the pixel is classified as 'insect'. Please note that every non-hydrometeor Cloudnet pixel which exceeds this threshold is called 'insect'. In reality, point targets other than insects, e.g., debris or plant material, might also fall into that category. Thus, we are aware that this approach is likely overestimating the true number of insects. Whether this effect can be quantified, for example, if it is especially prominent for high surface wind speeds, will be evaluated in a follow-up paper.

2.4 | VOODOO

VOODOO is a retrieval based on deep convolutional neural networks mapping cloud radar Doppler spectra to the probability of presence of cloud droplets (Schimmel et al. 2022). In the original VOODOO application, the characteristic signatures of liquid droplets in the radar Doppler spectra are used to differentiate them from ice particles. In this study, the characteristic signatures of insects in the radar Doppler spectra will be used to differentiate them from hydrometeors. Radar Doppler spectra of insects are often distinguishable by eye from those of clouds, as insect-generated radar signals form sharp narrow peaks (Luke et al. 2008, Wood et al. 2009), while a particle size-distribution of hydrometeors results in broader peaks in the radar Doppler spectrum (Fig. 1).

The most important steps in creating the VOODOO retrieval will be briefly summarized in the following, however, for an in-depth description of the pre-processing steps necessary and the feature sampling the reader is referred to Schimmel et al. (2022). First, the total back-scattered signal is calculated as the sum of the received horizontally and vertically polarized radar signals. The noise floor is estimated using the method of Hildebrand and Sekhon (1974) and lower reflectivity values are removed from the stored radar Doppler spectra. To extract the spectral features, the number of Doppler bins is interpolated to 256 (default value) and the bins, in which reflectivity values were removed due to noise-filtering, are filled with the reflectivity value of the sensitivity limit. The spectral reflectivity values are then converted to dBZ and normalized between $S_{max} = 20$ dBZ and $S_{min} = -50$ dBZ. The Cloudnet labels in combination with the assigned normalized spectra generate the input data set. VOODOO exploits principles from image classification, as demonstrated in (Krizhevsky et al. 2017). The architecture of VOODOO includes multiple strided-convolutional layers for feature extraction and dense layers for classification. The output layer transforms the input from the final dense layer into a probability-like value ranging from 0 (no insects present) to 1 (insects present). Finally, a threshold is applied to distinguish between non-insect and insect predictions. In this study, we consider pixels with an insect probability above 0.5 as insect.

The advantage of using VOODOO to estimate the insect probability over using the Cloudnet classification labels is that VOODOO avoids empirically chosen thresholds. These thresholds are fixed within Cloudnet, however, they can be different for different sites or radar instrument configurations. Contrarily, the characteristic signatures of insects in the radar Doppler spectra, which are the basis of insect detection in VOODOO, are expected to be consistent.

2.5 | PEAKO

If only one insect is present in a radar range bin, its signature in the Doppler spectrum can be easily identified, because it only causes one Doppler peak. However, in summertime conditions, typically multiple insects are present in the radar observation volume (e.g., for LIMRAD94 at 12 m vertical resolution in 200 m altitude, about 30 m³), causing a superposition of multiple sharp narrow peaks in the Doppler spectrum (Luke et al. 2008, Williams et al. 2021), as illustrated in Fig. 1. The supervised learning radar Doppler spectra peak-finding algorithm PEAKO (Kalesse et al. 2019) is used to investigate the characteristics of present peaks, even if they are not separated by the noise floor. Initially developed to determine the number of hydrometeor types in a certain cloud volume, PEAKO is a supervised machine learning approach trained on at least 200 radar Doppler spectra for each chirp section of LIMRAD94 (see Tab. 1). The training provides a set of parameters used to identify peaks in the typically noisy Doppler spectra for the specific cloud radar settings used. The six adjustable parameters are thresholds for peak width and prominence, number of time and range averages and the span and polynomial order for smoothing (Vogl et al. 2024). The parameters leading to the highest similarity with the user-defined training data set are saved in a configuration file and can be used as input for peakTree. More details of the PEAKO algorithm are introduced and demonstrated in Kalesse et al. (2019) and Vogl et al. (2024).

2.6 | peakTree

The peakTree algorithm is used to identify, organize and interpret the peaks in radar Doppler spectra (Radenz et al. 2019). It provides a recursive list of all subpeaks in the spectrum without a priori assumptions on their structure. These subpeaks are then characterized by their mean Doppler velocity, reflectivity, spectral width, skewness, prominence and LDR. In its latest release peakTree has been made compatible with PEAKO and can directly utilize the PEAKO training parameters via a configuration file (Vogl et al. 2024). Although peakTree inherently provides the option to select specific hydrometeor types with threshold based rules, it does not yet differentiate between hydrometeors and biological targets, such as insects. In this study, only information about the number of Doppler spectrum peaks is used. As we assume that one peak refers to a single insect, the number of peaks directly refers to the number of insects present in each radar bin. Future work will explore the opportunities granted by the additional peak-specific variables provided by peakTree.

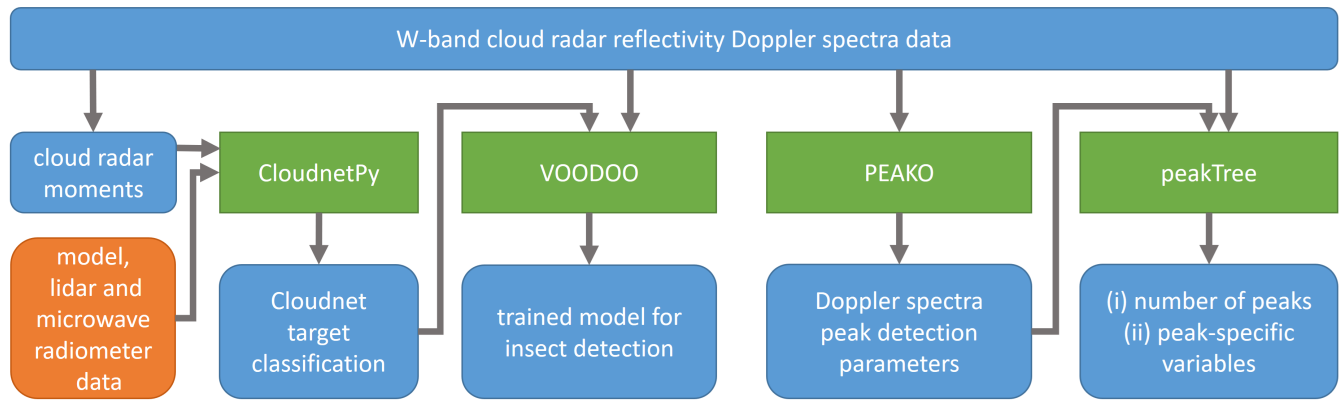


FIGURE 2 LIMRAD94 data processing flow chart for aerial insect detection. Blue boxes represent used data sets, green boxes depict software tools and the orange box represents the additional data sets, which are necessary for CloudnetPy processing, but are not discussed further in this paper.

3 | METHODOLOGY

3.1 | Combining the radar data processing techniques

This section shows how we combine the different established radar processing techniques introduced in detail in the previous sections to apply on LIMRAD94 data. Figure 2 depicts the sequence of these methods as applied in this work. Our approach at all steps of the processing chain is to ensure a high reliability of our data being insects. To achieve that goal the data filtering was rather strict and conservative.

First, CloudnetPy generates the target classification product based on the cloud radar moments (reflectivity, mean Doppler velocity and spectral width), weather model data and lidar data. The target labels are used in addition to the cloud radar reflectivity spectra for the training of VOODOO. However, a review of the extensive data set has shown that the CloudnetPy target classification sometimes gives unrealistic results at the edges of clouds and precipitation, where pixels are erroneously labeled as insects (Kalesse-Los et al. 2023). It is unclear whether this is due to partial beam filling or uncharacteristically low reflectivity values for liquid targets, but these obvious misclassifications are removed for the data analysis. The applied filtering algorithm removes pixels containing insects, which directly border pixels containing liquid water in either the time or range dimension. From the location of the thereby selected pixels, two bins in each direction of the two dimensions, i.e., two range gates up and down and two time steps before and after, are masked and, thus, not considered for the subsequent analysis.

Afterwards, VOODOO is trained on a subset of the remaining pixels. The labeled training data set has to contain sufficiently large samples of input (Doppler radar spectra) and output (CloudnetPy classification labels) to ensure a reliable insect detection model (Schimmel et al. 2022). The insect detection model is then applied to the rest of the valid pixels to predict the probability that these pixels contain insects. A threshold of 50 % insect probability was used for this study, every pixel with a lower insect probability is masked.

To extract information about the number of insects in each pixel, the Doppler spectra are processed further with PEAKO and peakTree. It is assumed that every narrow peak in the radar Doppler spectrum of each pixel identified by VOODOO as 'insect' represents one insect (Wood et al. 2009). PEAKO needs a sub set of the radar Doppler spectra for the training of the algorithm. Subsequently, the optimal parameters for the peak detection found by PEAKO are used to apply peakTree on the remaining data set. Finally, peakTree yields the location and characteristics of the peaks in the LIMRAD94 radar Doppler spectra.

3.2 | Comparison of radar instruments

An opportunity for comparison is presented by observations of the MR1 bird radar in Bad Lauchstädt (Sect. 2.2). As there are significant hardware differences between the two radars and they are located 40 km from each other, it is not expected that the insect concentration values agree perfectly. The most prominent difference between both instruments is the wavelength, which

differs by a factor of 10 (LIMRAD94: 0.32 cm, MR1: 3.2 cm). As radars are most sensitive to targets that are comparable in size to their wavelength, LIMRAD94 more reliably observes smaller targets, like aphids or mosquitoes. However, for targets larger than the radar wavelength - like large aerial insects in the cm size range - the Rayleigh scattering assumption is not valid anymore. Instead scattering follows the Mie regime, for which the reflectivity is not relative to the radar cross section of the target anymore. The MR1 can more confidently observe larger insects, e.g., moths, not being sensitive to small ones in the mm-size range. Another difference between both instruments is the beam width (LIMRAD94: 0.48°, MR1: 17.5°). As an example, at 200 m altitude, the diameters of the observation volumes would be about 2 m for LIMRAD94 and approximately 60-100 m for MR1 (depending on the size of the insect; Schmid et al. 2019). Consequently, MR1 has a much larger observation volume (MR1: >22000 m³, LIMRAD94: 30 m³), which can be an advantage in situations with low insect concentration. If insects are rather sparsely distributed, the narrow beam of LIMRAD94 might miss them, while the MR1 might detect their occurrence. For the MR1, it is not possible to discern whether one or multiple insects have been detected in one pixel, even though the detected radar cross section for multiple insects might be larger than for a single one. Additionally, the MR1 slightly underestimates the insect concentration values at higher altitudes, because the sensitivity of the instrument is strongly dependent on the insect size (Schmid et al. 2019), resulting in potentially increasing numbers of insects being missed merely due to their smaller size. There are only a few data points above 500 m at all times of the day detected by the MR1. This can be due to the instrument sensitivity being too low at these altitudes or the larger insects, which are detected by the MR1, not flying that high regularly. Therefore, MR1 measurements from altitudes above 500 m will not be considered in the subsequent analysis. It is expected that LIMRAD94 observes higher absolute numbers of flying insects for the above-mentioned reasons.

An additional contributing factor to different absolute insect concentrations and diel timings can be the location of the sites (e.g., Knop et al. 2023, Haest et al. 2024b). The site of the MR1 in Bad Lauchstädt is rather rural. While Leipzig with a population of around 600000 inhabitants represents an urban environment, the location of LIMRAD94 at TROPOS in the outskirts of Leipzig can be considered suburban.

For a meaningful comparison, both data sets have been interpolated to the same grid. For convenience in processing time, we compare the output of both radars at a vertical resolution of 50 m and temporal resolution of 1 h, providing ample detail for the assessment and interpretation of biological meaning of the observed patterns. The highest absolute value of simultaneously observed insects during each hour of LIMRAD94 measurements has been used to compare to the hourly derived values of the MR1. The comparison period consists of one month of data between 1 June 2022 and 30 June 2022. For comparability, the radar-derived aerial insect concentrations from both instruments have been upscaled to number of insects per km³. Overestimations of insect concentration can occur if insect plumes would occur more frequently over the radar instrument than in other parts of the km³ volume, which we consider unlikely though. As the absolute numbers of both instruments most likely will not agree due to the different used wavelengths and, thus, the different detected targets, we also compare biologically relevant statistics, such as the diel flight timing of the insects. For that, the data sets are normalized. For each radar instrument, the mean insect concentration values for each hourly interval and each altitude over the comparison period are calculated. These values are then divided by the maximum of the insect concentration at each altitude to yield the mean normalized insect concentration.

4 | RESULTS AND DISCUSSION

4.1 | Aerial insect concentration

First, the mean diel cycle of the absolute insect concentration numbers is compared between both instruments. As a reference, Fig. 3 a) and b) show the absolute insect concentration numbers derived from LIMRAD94 and the MR1, respectively. For both instruments, most insects are detected close to the ground and the absolute number of detected insects is decreasing with altitude. It is evident that LIMRAD94 detects three to five orders of magnitudes more insects than the MR1, which is possibly caused by the different wavelengths being sensitive to differently-sized insects. For LIMRAD94 (Fig. 3a) the diel variation at each altitude is not very discernible, as the variation within one altitude layer is lower (less than one order of magnitude) than the variation in the vertical profile (around two orders of magnitude). In contrast, the absolute insect concentration of the MR1 (Fig. 3b) shows some more diel variation within one altitude layer. In the following, the values of both data sets have been normalized to improve the comparability.

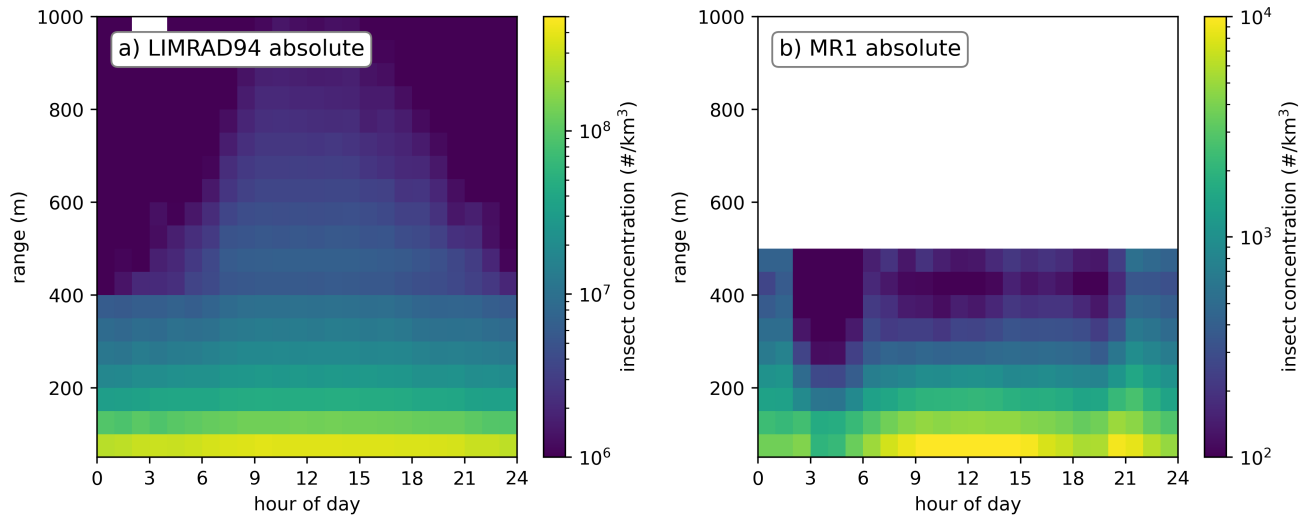


FIGURE 3 Mean insect concentration for each hourly slice over pixels where insects are identified for the comparison period 1 June 2022 to 30 June 2022. a) and b) show the mean of the absolute values derived from LIMRAD94 and MR1 radar instruments, respectively.

4.2 | Diel insect phenology

Figure 4 a) and b) show the distribution of the diel cycle in different altitudes for both radar instruments. For LIMRAD94 (Fig. 4a), observed vertical profiles of flying insect concentration generally follow the evolution of the atmospheric boundary layer (ABL). The height of the ABL is not constant, but follows a regular cycle on typical fair weather days. The ABL is most distinct during the day, when thermal convection and turbulent mixing is high, enabling passive transport of airborne particles to higher altitudes. During the night, the ABL is generally stable. For range gates close to the ground, the variation of the insect concentration in LIMRAD94 data during the day is not very pronounced. It ranges from 0.65 during the night to 0.95 in the late morning. The normalized insect concentration in the first range gate stays above 0.95 for several hours between 8 and 16 UTC before it decreases again. At altitudes above 400 m, the nighttime minimum of insect concentration becomes more pronounced, dropping to around 0.2 at 23 to 1 UTC. For the highest considered range gate at 975 m, the insect concentration during the night drops below 0.05 between hours 22 to 3 UTC, while the maximum is at 10 UTC. These results are in line with the only previous study (Wood et al. 2009) using W-band to characterize diel flight patterns.

The mean diel variation of larger insects derived from MR1 data (Fig. 4b) at the lowest range gate (75 m) has its maximum during day time, in a similar pattern as LIMRAD94. The lowest values of about 0.2 occur between 3 - 4 UTC while maximum values are reached at 12 UTC (i.e. shortly after local noon). However, in the MR1 data, a second maximum is found at dusk, although the values are slightly lower (around 0.9) than at noon. Higher up, the maximum at dusk becomes even more pronounced than the maximum at noon. For all range gates above the first, the maximum at dusk constitutes the daily maximum at the respective altitude. This pattern in the MR1 insect data is similar as was described in Haest et al. (2024b) for data from 17 vertically looking MR1 radars across Europe. For altitudes up to 300 m there is still an increase in normalized insect concentration during daytime, but the highest values are observed between 21 and 2 UTC with a sudden drop to the minimum between 2 and 5 UTC. However, it has to be stated that the absolute values of insect concentration decrease with altitude for both instruments for all times of the day (Fig. 3a and b), similar to what is most often observed (e.g., Hu et al. 2016). It is only after normalizing with the altitude-specific maximum that the values appear higher than those close to the ground.

The differences in where and when insects are detected by both instruments are affected by the different instrument characteristics. Small insects tend to fly higher, because they are lighter and, thus, can more easily exploit updrafts in the atmospheric boundary layer (Geerts and Miao 2005, Helms et al. 2016). In the evening and during the night, thermal updrafts cease and insect concentration in LIMRAD94 data decreases, especially at higher layers. In the lower atmospheric boundary layer below 300 m, insect concentration detected by LIMRAD94 does not drop below 0.6 even during the night. This indicates that a lot of small insects still fly during the night, although they cannot get to higher altitudes themselves. That the relative

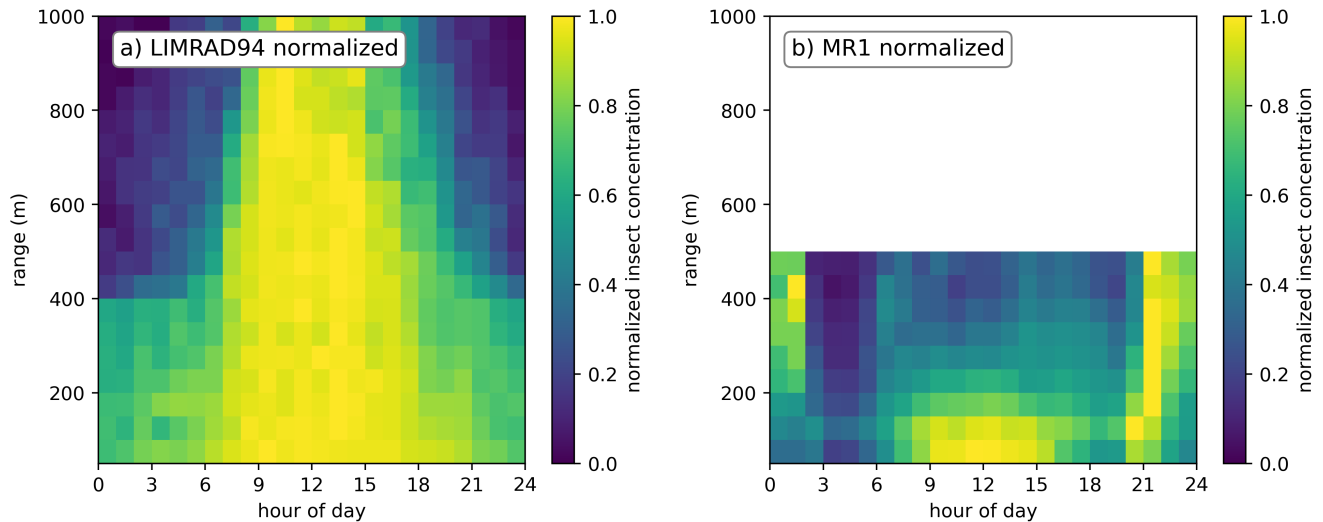


FIGURE 4 Mean normalized insect concentration for each hourly slice over pixels where insects are identified for the comparison period 1 June 2022 to 30 June 2022. a) and b) show the mean of the per altitude normalized values derived from LIMRAD94 and MR1 radar instruments, respectively.

number of small flying insects decreases during the night, fits with the common observation of higher average insects sizes during nocturnal aerial movements (Haest et al. 2024b). Larger insects are able to fly without the support of thermal convection and were detected up to 500 m, even at night.

4.3 | Correlation between both radar instruments

To explore the correlation between both data sets in more detail, Fig.5 shows the Pearson correlation coefficient for four time periods of the day. The day is divided into crepuscular morning (1.00 - 2.59 UTC), day (3.00 - 18.59 UTC), crepuscular evening (19.00 - 20.59 UTC) and night (21.00 - 0.59 UTC), similar to Haest et al. (2024b). The correlation coefficient R is shown in the legend of Fig. 5. For all four defined periods of the day, the correlation coefficient is above 0.8, indicating a strong correlation between the data sets. The correlation is particularly strong during the day and crepuscular evening ($R=0.86$) and least strong in crepuscular morning.

Bauer et al. (2024) define 'abundance and biomass estimates' as an essential biodiversity variable. Although the absolute values of detected insect concentrations by both instruments differ by several orders of magnitude, we investigated whether the ratio of detected insect concentrations between both measurements is constant through time and height. If this relationship would be relatively constant, it would enable the transfer of observations from one radar instrument to the other, i.e., enabling the estimation of the number of smaller insects using insect concentrations derived by X-Band and the estimation of the number of larger insects using W-Band measurements. In the following, the ratio between both data sets is referred to as 'scaling factor' for different times of the day.

Figure 6 shows the mean scaling factor between the absolute aerial insect concentration values of LIMRAD94 and MR1 up to an altitude of 500 m. Since the absolute values derived from LIMRAD94 data (see Fig. 3a) do not vary much in this altitude range, the scaling factor between both instruments is similar in appearance to the absolute values of the MR1 (Fig. 3b).

With values of about 180000 to 810000, the scaling factor is highest during the early hours of the day (3 to 6 UTC) up to around 400 m. At this time of the diel cycle the MR1 detects the least insects, thus, the scaling factor is high. With values of about 4000 to 38000, the ratio is lowest at dusk, when the MR1 detects its maximum of insects. At altitudes above 350 m between 21 and 2 UTC the number of insects detected by LIMRAD94 decreases because not many small insects reach these altitudes. However, the larger insects detected by the MR1 are flying throughout the night, even at these altitudes. Therefore, the scaling factor has another minimum during this time and altitude range.

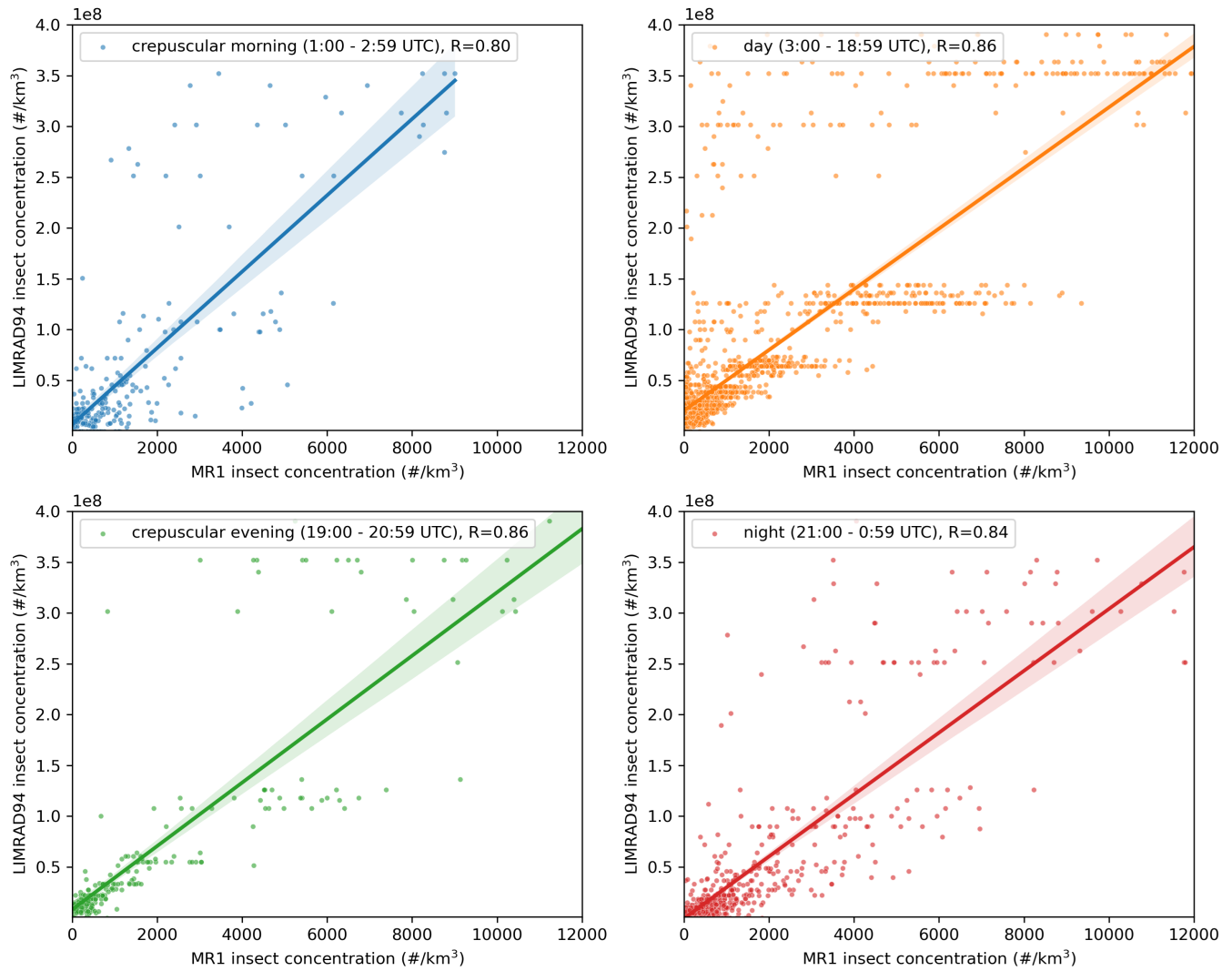


FIGURE 5 Scatterplot of absolute insect concentration values of LIMRAD94 (y-axis) vs. MR1 (x-axis) and correlation coefficient for four time periods of the day as indicated in the plot legends.

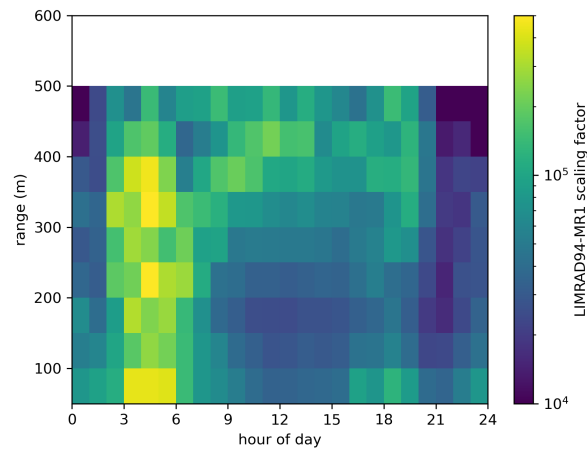


FIGURE 6 Mean ratio between absolute number concentration derived from LIMRAD94 data and MR1 data ('scaling factor').

5 | SUMMARY, CONCLUSIONS AND OUTLOOK

This paper discussed the combination of several state-of-the-art radar data processing techniques to achieve novel results in the detection of insects using a cloud radar with small wavelength, which is most sensitive to mm-sized insects. It has been shown how to effectively use the machine learning approach VOODOO to detect insects from Doppler radar spectra. This feature-based detection method does not depend on empirically chosen thresholds - like the other introduced target classification processing tool CloudnetPy does - and should be applicable to different sites, which needs to be investigated in a follow-up publication. Subsequently, the VOODOO-based detection mask was used to extract insect signals from Doppler radar spectra to apply the peak-finding algorithms PEAKO and peakTree.

With the assumption that every narrow Doppler spectrum peak is caused by a single insect, insect concentration values were calculated for LIMRAD94 and studied along with insect concentration data from a BirdScan MR1 radar for June 2022 in central Germany. Given that radars are most sensitive to targets comparable in size to their wavelength, it is presumed that both instruments observe different groups of aerial insect fauna, as their wavelength differ by a factor of 10 (LIMRAD94: 0.32 cm, MR1: 3.2 cm). The insect concentration values derived by both radars, thus, help to identify and compare flight behaviour between smaller and larger insects. Knowledge about the flight timing and flight altitude of small insects derived from LIMRAD94 data expands and fills in certain data gaps with additional information on a different subset of aerial fauna.

We demonstrated that the absolute aerial insect concentration detected by LIMRAD94 is about three to five orders of magnitude higher than the values derived from MR1 data. This difference is caused by LIMRAD94 being able to detect small flying insects, e.g., aphids or mosquitoes, which are far more numerous in the atmosphere than large insects (Hu et al. 2016). For smaller insects, a clear dependence of the insect concentration on the evolution of the atmospheric boundary layer is evident. The maximum of diel insect flight for all considered altitudes is reached approximately at noon local time. Below 400 m, insect concentration is still noticeably high at night, dropping to about 50 % to 60 % of the altitudinal maximum value. However, above 500 m, insect concentration decreases more strongly during the night, reduced to below 5 % in the highest considered range gate in 975 m from 22 UTC to 3 UTC. Thus, it is concluded that small insects need the help of (thermal) convection during daytime to reach altitudes above a few hundred meters.

The MR1 is not very suited to detect mm-sized insects and, thus, the data obtained with it better describe the activity of larger insects, like moths. In contrary to LIMRAD94 data, for larger insects, there are two (and sometimes three) maxima of insect flight over the course of the day. The second maximum of diel insect flight is found by MR1 at night from 21 UTC to 2 UTC in all altitudes above the lowest range gate of 50 m. Since this second maximum is only evident in MR1 data, it is presumed that it consists predominately of larger, nocturnal insects. Across all altitudes, the least flying insects are detected by the MR1 between 3 UTC and 5 UTC.

Although the groups of detected insects differ between both instruments, the two data sets correlate strongly. For the analysis of correlation, the data were split into four diel phases (night, crepuscular morning, day and crepuscular evening) and evaluated separately. The Pearson correlation coefficients for all four phases are above 0.8.

This study introduced the methodology of deriving aerial insect concentration values from spectral W-band Doppler cloud radar data and the application on a rather short data set. A subsequent study will apply this approach to a continuous 15 months data set of observations performed on the roof platform of the Leipzig University Institute for Meteorology (LIM, 51°20' N, 12°22' E) in the city center of Leipzig from 18 December 2020 to 6 March 2022. This larger data sets also presents the opportunity to evaluate the potential dependence of aerial insect concentration and diel flight timing on environmental factors, e.g., surface wind speed or air temperature.

In this work, a comparison between the data of the two radar instruments LIMRAD94 and MR1 was performed. However, we acknowledge that the conditions of this comparison were not ideal, as the instruments operated with different settings and at different locations about 40 km apart. In the future, a collocated measurement period with both instruments at the same location and operating with similar observation settings would be beneficial to help support the findings of this study.

Additionally, the radar Doppler spectrum peaks detected by the peakTree algorithm have not been investigated in great detail so far. For this first introduction of the methods, only the total number of peaks has been analyzed. However, peakTree offers the opportunity to determine radar variables, e.g., reflectivity, mean Doppler velocity and spectral width, for every detected sub peak of the radar Doppler spectrum. This information provides the possibility to characterize the individual insects detected even further and perhaps differentiate between various sub-groups of them.

Finally, the application of this approach to other cloud radar instruments at other locations can be considered. There are several 94 GHz cloud radars operational in Europe for meteorological applications, which usually have their data publicly available.

Applying the methods presented in this study to multi-year data sets may provide an opportunity to study trends in aerial insect behaviour with high temporal and vertical resolution.

DATA AVAILABILITY STATEMENT

The data that support the findings of this study are available from the corresponding author upon reasonable request.

CONTRIBUTIONS BY THE AUTHORS

ML was the primary author of this paper, did most of the data analysis and prepared the manuscript. HKL helped greatly in interpreting results and preparing the manuscript. BH provided the processed BirdScan MR1 data set and important help in interpreting entomological results. TV conducted the PEAKO and peakTree training of the data set and provided help in interpreting results. RvK helped ML with the entomological analysis of the results. FA and MM helped in interpreting results and gave suggestions for the preparation of the manuscript. WS helped in conducting VOODOO model training and predictions. JQ and CW helped in defining research questions and provided general guidance during the project.











COMPETING INTERESTS

The authors declare that they have no conflict of interest.

ACKNOWLEDGMENTS

This work was funded by the Saxon State Ministry for Science, Culture and Tourism (SMWK) – [3-7304/44/4-2023/8846]. RvK was funded by the DFG (FZT 118). We thank Martin Radenz (TROPOS) for his work on peakTree and his help in the analysis of peakTree results.

ORCID

Moritz Lochmann  <https://orcid.org/0000-0002-4938-328X>,
Heike Kalesse-Los  <https://orcid.org/0000-0001-6699-7040>,
Birgen Haest  <https://orcid.org/0000-0002-8739-6460>,
Teresa Vogl  <https://orcid.org/0000-0002-6696-4967>,
Roel van Klink  <https://orcid.org/0000-0002-8125-1463>,
Freya Addison  <https://orcid.org/0000-0001-8439-290X>,
Maximilian Maahn  <https://orcid.org/0000-0002-2580-9100>,
Willi Schimmel  <https://orcid.org/0000-0001-8428-6445>,
Christian Wirth  <https://orcid.org/0000-0003-2604-8056>,
Johannes Quaas  <https://orcid.org/0000-0001-7057-194X>

REFERENCES

- Bauer, S., Tielens, E.K. & Haest, B. (2024) Monitoring aerial insect biodiversity: A radar perspective. *Philosophical Transactions of the Royal Society B: Biological Sciences*, 379(1904), 20230113. doi:10.1098/rstb.2023.0113.
- Boero, L., Poffo, D., Damino, V., Villalba, S., Barquez, R.M., Rodríguez, A. et al. (2020) Monitoring and Characterizing Temporal Patterns of a Large Colony of *Tadarida brasiliensis* (Chiroptera: Molossidae) in Argentina Using Field Observations and the Weather Radar RMA1. *Remote Sensing*, 12(2), 210. doi:10.3390/rs12020210.
- Cai, J., Yuan, Q., Wang, R., Liu, C. & Zhang, T. (2019) Insect detection and density estimation based on a Ku-band scanning entomological radar. *The Journal of Engineering*, 2019(21), 7636–7639. doi:10.1049/joe.2019.0600.
- Chapman, J.W., Drake, V.A. & Reynolds, D.R. (2011) Recent Insights from Radar Studies of Insect Flight. *Annual Review of Entomology*, 56(Volume 56, 2011), 337–356. doi:10.1146/annurev-ento-120709-144820.

- Chen, H., Li, M., Månefjord, H., Travers, P., Salvador, J., Müller, L. et al. (2024) Lidar as a potential tool for monitoring migratory insects. *iScience*, 27(5), 109588. doi:10.1016/j.isci.2024.109588.
- Drake, V.A., Chapman, J.W., Lim, K.S., Reynolds, D.R., Riley, J.R. & Smith, A.D. (2017) Ventral-aspect radar cross sections and polarization patterns of insects at X band and their relation to size and form. *International Journal of Remote Sensing*, 38(18), 5022–5044. doi:10.1080/01431161.2017.1320453.
- Drake, V.A. & Reynolds, D.R. (2012) *Radar Entomology: Observing Insect Flight and Migration*. : CABI.
- Gao, B., Wotton, K.R., Hawkes, W.L.S., Menz, M.H.M., Reynolds, D.R., Zhai, B.P. et al. (2020) Adaptive strategies of high-flying migratory hoverflies in response to wind currents. *Proceedings of the Royal Society B: Biological Sciences*, 287(1928), 20200406. doi:10.1098/rspb.2020.0406.
- Geerts, B. & Miao, Q. (2005) Airborne Radar Observations of the Flight Behavior of Small Insects in the Atmospheric Convective Boundary Layer. *Environ Entomol*, 34(2), 361–377. doi:10.1603/0046-225X-34.2.361.
- Giuntini, S., Saari, J., Martinoli, A., Preatoni, D.G., Haest, B., Schmid, B. et al. (2024) Quantifying nocturnal thrush migration using sensor data fusion between acoustics and vertical-looking radar. *Remote Sensing in Ecology and Conservation*, n/a(n/a). doi:10.1002/rse2.397.
- Haest, B., Hertner, F., Schmid, B., Preatoni, D., De Groeve, J. & Liechti, F. (2024) *birdscanR: Migration Traffic Rate Calculation Package for Birdscan MRI Radars*. Zenodo.
- Haest, B., Liechti, F., Hawkes, W.L., Chapman, J., Åkesson, S., Shamoun-Baranes, J. et al. (2024) Continental-scale patterns in diel flight timing of high-altitude migratory insects. *Philosophical Transactions of the Royal Society B: Biological Sciences*, 379(1904), 20230116. doi:10.1098/rstb.2023.0116.
- Haest, B., Stepanian, P.M., Wainwright, C.E., Liechti, F. & Bauer, S. (2021) Climatic drivers of (changes in) bat migration phenology at Bracken Cave (USA). *Global Change Biology*, 27(4), 768–780. doi:10.1111/gcb.15433.
- Hallmann, C.A., Sorg, M., Jongejans, E., Siepel, H., Hoffland, N., Schwan, H. et al. (2017) More than 75 percent decline over 27 years in total flying insect biomass in protected areas. *PLOS ONE*, 12(10), e0185809. doi:10.1371/journal.pone.0185809.
- Helms, J.A., Godfrey, A.P., Ames, T. & Bridge, E.S. (2016) Predator foraging altitudes reveal the structure of aerial insect communities. *Sci Rep*, 6(1), 28670. doi:10.1038/srep28670.
- Hildebrand, P.H. & Sekhon, R.S. (1974) Objective Determination of the Noise Level in Doppler Spectra. *Journal of Applied Meteorology and Climatology*, 13(7), 808–811. doi:10.1175/1520-0450(1974)013<0808:ODOTNL>2.0.CO;2.
- Hu, G., Lim, K.S., Horvitz, N., Clark, S.J., Reynolds, D.R., Sapir, N. et al. (2016) Mass seasonal bioflows of high-flying insect migrants. *Science*, 354(6319), 1584–1587. doi:10.1126/science.aah4379.
- Illingworth, A.J., Hogan, R.J., O’Connor, E.J., Bouniol, D., Brooks, M.E., Delanoé, J. et al. (2007) Cloudnet: Continuous Evaluation of Cloud Profiles in Seven Operational Models Using Ground-Based Observations. *Bulletin of the American Meteorological Society*, 88(6), 883–898. doi:10.1175/BAMS-88-6-883.
- Kalesse, H., Vogl, T., Paduraru, C. & Luke, E. (2019) Development and validation of a supervised machine learning radar Doppler spectra peak-finding algorithm. *Atmospheric Measurement Techniques*, 12(8), 4591–4617. doi:10.5194/amt-12-4591-2019.
- Kalesse-Los, H., Kötsche, A., Foth, A., Röttenbacher, J., Vogl, T. & Witthuhn, J. (2023) The Virga-Sniffer – a new tool to identify precipitation evaporation using ground-based remote-sensing observations. *Atmospheric Measurement Techniques*, 16(6), 1683–1704. doi:10.5194/amt-16-1683-2023.
- Knop, E., Grimm, M.L., Korner-Nievergelt, F., Schmid, B. & Liechti, F. (2023) Patterns of high-flying insect abundance are shaped by landscape type and abiotic conditions. *Sci Rep*, 13(1), 15114. doi:10.1038/s41598-023-42212-z.
- Krizhevsky, A., Sutskever, I. & Hinton, G.E. (2017) ImageNet classification with deep convolutional neural networks. *Commun. ACM*, 60(6), 84–90. doi:10.1145/3065386.
- Küchler, N., Kneifel, S., Löhnert, U., Kollias, P., Czekala, H. & Rose, T. (2017) A W-Band Radar–Radiometer System for Accurate and Continuous Monitoring of Clouds and Precipitation. *Journal of Atmospheric and Oceanic Technology*, 34(11), 2375–2392. doi:10.1175/JTECH-D-17-0019.1.
- Kwakye, S., Kalesse-Los, H., Maahn, M., Seifert, P., van Klink, R., Wirth, C. et al. (2023) Classification of flying insects in polarimetric weather radar using machine learning and aphid trap data. *Atmospheric Measurement Techniques Discussions*, 1–16. doi:10.5194/amt-2023-69.
- Lukach, M., Dally, T., Evans, W., Hassall, C., Duncan, E.J., Bennett, L. et al. (2022) The development of an unsupervised hierarchical clustering analysis of dual-polarization weather surveillance radar observations to assess nocturnal insect abundance and diversity. *Remote Sensing in Ecology and Conservation*, 8(5), 698–716. doi:10.1002/rse2.270.
- Luke, E.P., Kollias, P., Johnson, K.L. & Clothiaux, E.E. (2008) A Technique for the Automatic Detection of Insect Clutter in Cloud Radar Returns. *Journal of Atmospheric and Oceanic Technology*, 25(9), 1498–1513. doi:10.1175/2007JTECHA953.1.
- Mäkinen, T., Ritvanen, J., Pulkkinen, S., Weisshaupt, N. & Koistinen, J. (2022) Bayesian Classification of Nonmeteorological Targets in Polarimetric Doppler Radar Measurements. *Journal of Atmospheric and Oceanic Technology*, 39(10), 1561–1578. doi:10.1175/JTECH-D-21-0177.1.
- Montgomery, G.A., Belitz, M.W., Guralnick, R.P. & Tingley, M.W. (2021) Standards and Best Practices for Monitoring and Benchmarking Insects. *Front. Ecol. Evol.*, 8. doi:10.3389/fevo.2020.579193.
- Nilsson, C., Dokter, A.M., Verlinden, L., Shamoun-Baranes, J., Schmid, B., Desmet, P. et al. (2019) Revealing patterns of nocturnal migration using the European weather radar network. *Ecography*, 42(5), 876–886. doi:10.1111/ecog.04003.
- Radenz, M., Bühl, J., Seifert, P., Griesche, H. & Engelmann, R. (2019) peakTree: A framework for structure-preserving radar Doppler spectra analysis. *Atmospheric Measurement Techniques*, 12(9), 4813–4828. doi:10.5194/amt-12-4813-2019.
- Reynolds, D.R. & Riley, J.R. (2002) Remote-sensing, telemetric and computer-based technologies for investigating insect movement: A survey of existing and potential techniques. *Computers and Electronics in Agriculture*, 35(2), 271–307. doi:10.1016/S0168-1699(02)00023-6.
- Riley, J. (1985) Radar cross section of insects. *Proc. IEEE*, 73(2), 228–232. doi:10.1109/PROC.1985.13135.
- Riley, J.R. (1994) Flying insects in the field. In: Wratten, S.D. (Ed.) *Video Techniques in Animal Ecology and Behaviour*. DordrechtSpringer Netherlands, pp. 1–15.
- Schimmel, W., Kalesse-Los, H., Maahn, M., Vogl, T., Foth, A., Garfias, P.S. et al. (2022) Identifying cloud droplets beyond lidar attenuation from vertically pointing cloud radar observations using artificial neural networks. *Atmospheric Measurement Techniques*, 15(18), 5343–5366. doi:10.5194/amt-15-5343-2022.
- Schmid, B., Zaugg, S., Votier, S.C., Chapman, J.W., Boos, M. & Liechti, F. (2019) Size matters in quantitative radar monitoring of animal migration: Estimating monitored volume from wingbeat frequency. *Ecography*, 42(5), 931–941. doi:10.1111/ecog.04025.
- Schuch, S., Wesche, K. & Schaefer, M. (2012) Long-term decline in the abundance of leafhoppers and planthoppers (Auchenorrhyncha) in Central European protected dry grasslands. *Biological Conservation*, 149(1), 75–83. doi:10.1016/j.biocon.2012.02.006.

- Shaw, J.A., Seldomridge, N.L., Dunkle, D.L., Nugent, P.W., Spangler, L.H., Churnside, J.H. et al. Polarization lidar measurements of honeybees for locating buried landmines. In: *Polarization Science and Remote Sensing II*. Vol. 5888, Aug. 2005. : SPIE, pp. 197–203.
- Shi, X., Schmid, B., Tschanz, P., Segelbacher, G. & Liechti, F. (2021) Seasonal Trends in Movement Patterns of Birds and Insects Aloft Simultaneously Recorded by Radar. *Remote Sensing*, 13(9), 1839. doi:10.3390/rs13091839.
- Stepanian, P.M., Entekin, S.A., Wainwright, C.E., Mirkovic, D., Tank, J.L. & Kelly, J.F. (2020) Declines in an abundant aquatic insect, the burrowing mayfly, across major North American waterways. *Proceedings of the National Academy of Sciences*, 117(6), 2987–2992. doi:10.1073/pnas.1913598117.
- Thomas, J.A., Telfer, M.G., Roy, D.B., Preston, C.D., Greenwood, J.J.D., Asher, J. et al. (2004) Comparative Losses of British Butterflies, Birds, and Plants and the Global Extinction Crisis. *Science*, 303(5665), 1879–1881. doi:10.1126/science.1095046.
- Tielens, E.K. & Kelly, J. (2024) Temperature, not net primary productivity, drives continental-scale variation in insect flight activity. *Philosophical Transactions of the Royal Society B: Biological Sciences*, 379(1904), 20230114. doi:10.1098/rstb.2023.0114.
- Tukiainen, S., O'Connor, E. & Korpinen, A. (2020) CloudnetPy: A Python package for processing cloud remote sensing data. *Journal of Open Source Software*, 5(53), 2123. doi:10.21105/joss.02123.
- Van Doren, B.M. & Horton, K.G. (2018) A continental system for forecasting bird migration. *Science*, 361(6407), 1115–1118. doi:10.1126/science.aat7526.
- van Klink, R., Bowler, D.E., Gongalsky, K.B., Swengel, A.B., Gentile, A. & Chase, J.M. (2020) Meta-analysis reveals declines in terrestrial but increases in freshwater insect abundances. *Science*, 368(6489), 417–420. doi:10.1126/science.aax9931.
- Vogl, T., Radenz, M., Ramelli, F., Gierens, R. & Kalesse-Los, H. (2024) PEAKO and peakTree: Tools for detecting and interpreting peaks in cloud radar Doppler spectra – capabilities and limitations. *EGUsphere*, 1–31. doi:10.5194/egusphere-2024-837.
- Wainwright, C.E., Volponi, S.N., Stepanian, P.M., Reynolds, D.R. & Richter, D.H. (2023) Using cloud radar to investigate the effect of rainfall on migratory insect flight. *Methods in Ecology and Evolution*, 14(2), 655–668. doi:10.1111/2041-210X.14023.
- Weissaupt, N., Hervo, M. & Haest, B. (2023) Comparison of bird migration in a radar wind profiler and a dedicated bird radar. *Remote Sensing in Ecology and Conservation*, 9(6), 820–828. doi:10.1002/rse2.350.
- Weissaupt, N., Lehmann, V., Arizaga, J. & Maruri, M. (2017) Radar wind profilers and avian migration - a qualitative and quantitative assessment verified by thermal imaging and moon watching. *Methods in Ecology and Evolution*, 8. doi:10.1111/2041-210X.12763.
- Werber, Y., Sextin, H., Yovel, Y. & Sapir, N. (2023) BATScan: A radar classification tool reveals large-scale bat migration patterns. *Methods in Ecology and Evolution*, 14(7), 1764–1779. doi:10.1111/2041-210X.14125.
- Williams, C.R., Johnson, K.L., Giangrande, S.E., Hardin, J.C., Öktem, R. & Romps, D.M. (2021) Identifying insects, clouds, and precipitation using vertically pointing polarimetric radar Doppler velocity spectra. *Atmospheric Measurement Techniques*, 14(6), 4425–4444. doi:10.5194/amt-14-4425-2021.
- Wood, C.R., O'Connor, E.J., Hurley, R.A., Reynolds, D.R. & Illingworth, A.J. (2009) Cloud-radar observations of insects in the UK convective boundary layer. *Meteorological Applications*, 16(4), 491–500. doi:10.1002/met.146.
- Zhang, T., Liu, X., Hu, C., Wang, R., Liu, C. & Li, W. (2019) Insect wing-beat frequency automatic extraction and experimental verification with a Ku-band insect radar system. *The Journal of Engineering*, 2019(21), 7973–7976. doi:10.1049/joe.2019.0653.